



Energy-efficient design of a carbon fiber-based self-heating concrete pavement system through finite element analysis

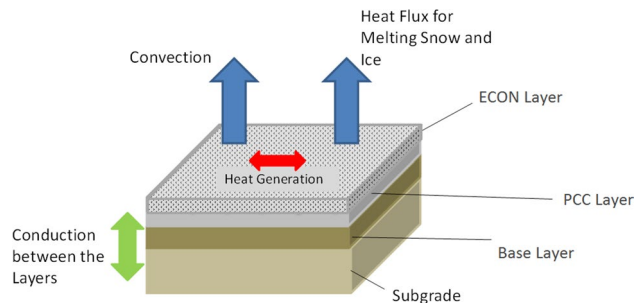
S. M. Sajed Sadati¹ · Kristen S. Cetin² · Halil Ceylan^{3,4} · Sunghwan Kim⁵

Received: 12 February 2020 / Accepted: 30 April 2020 / Published online: 18 May 2020
© Springer-Verlag GmbH Germany, part of Springer Nature 2020

Abstract

Electrically conductive concrete (ECON) heated pavement system (HPS) is a newly developed clean technology to reduce the use of polluting chemicals for removal of snow and ice. This technology requires further comprehensive studies for achieving an energy-efficient design. To construct an energy-efficient system, ECON HPS design includes determining the most appropriate configuration of electrodes embedded in the ECON layer. The spacing, shape and dimensions of these electrodes are important design factors impacting the thermal and energy performance of the system. While field tests are resource-intensive, the use of numerical modeling can complement such experimental tests to provide a better overall understanding of the technology's behavior. In this paper, the thermal and energy performance of ECON HPS is investigated through considering various system configuration designs, with an experimentally validated finite element model. A performance index is defined for comparing both thermal and energy performance of the configurations to obtain an energy-efficient design. The results indicate that a configuration with six circular electrodes at 100 cm spacing exhibited the best performance index and the highest energy efficiency. Since a test section with higher performance index would be capable of achieving a higher average surface temperature for the same energy input, such a section would have higher efficiency compared to other sections evaluated. This analysis results in narrowing down the ECON HPS's configuration design options before performing experimental tests.

Graphic abstract



Keywords Airport sustainability · Energy efficiency · Electrically conductive concrete · Heated pavement systems · Finite element analysis

Introduction

Methods used for the construction and operation of the transportation infrastructure are continuously improving through ongoing research focused on achieving cleaner technologies and higher resiliency under harsh weather conditions (Voskamp and de Ven 2015; Jiang et al. 2018; Sadati et al.

✉ Kristen S. Cetin
cetinkri@msu.edu

Extended author information available on the last page of the article

2018). The performance of transportation hubs such as airports during adverse winter weather is an important aspect of research in this area. Severe winter weather conditions can adversely impact accessibility to international and domestic hubs, resulting in potentially severe economic consequences during significant snowfall events (Anand et al. 2014).

Background

Current practice for snow and ice removal during winter weather events typically includes the use of a combination of snow- and ice-melting chemicals and snow-plowing equipment, and such practices introduce pollutants to the environment, consume a considerable amount of resources, can be time-intensive, and also can contribute to flight delays (Anand et al. 2014; Abdulla et al. 2018). Using such chemicals can contaminate runoff water, and emissions from the plowing equipment adversely affect the air quality at the airport (Fay et al. 2015); therefore, the development and implementation of cleaner technologies are needed to continue to keep airports accessible under harsh winter weather conditions. One of the technologies that could considerably enhance performance of airports during snowfall events in cold regions is heated pavement systems (HPSs) (Anand et al. 2014). This technology helps with reducing the use of chemicals for snow and ice removal and provides a faster and more convenient method for such operations (Sassani et al. 2018). Reducing the use of deicing chemicals could also improve the service life of concrete pavements since such chemicals adversely affect the durability of concrete materials (Amini et al. 2019). Since portland cement concrete (PCC) is extensively used as a construction material, producing it with less environmental impacts is a necessity for sustainable development. For example, modifying the concrete mix to produce more sustainable materials by enabling the use of different types of waste is already introduced as a promising method (Shamsaei et al. 2019). The most recent development in HPS technology is the use of electrically conductive material in concrete mix design, combined with the application of a voltage across the concrete to generate heat through resistive heating (Abdulla et al. 2018). Although PCC normally has a very high electrical resistivity (Malakooti 2017; Malakooti et al. 2018), when electrically conductive materials are added to its mix, it can be used for resistive heating applications (Sassani et al. 2018). Figure 1 is a schematic diagram of an electrically conductive concrete (ECON) system representing a simplified configuration of this type of HPS in which a pair of electrodes connected to the electrical source establishes an electric potential gradient throughout the ECON material.

To evaluate ECON HPS performance in the field, test slabs fabricated by adding chopped carbon fibers to the concrete mix have been tested at the Des Moines International

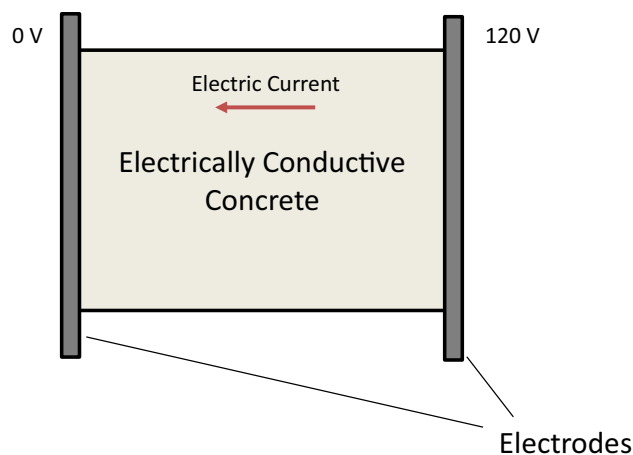


Fig. 1 Simplified schematic of an electrically conductive concrete heated pavement system

Airport (DSM) located in Iowa in the USA (ASHRAE Climate Zone 5A (ASHRAE 2007)). These slabs were constructed in October 2016 and have been tested throughout a range of snowfall events since their installation (Abdulla et al. 2016). These were designed using six angle iron stainless steel electrodes. This initial design was based on tests performed in a controlled laboratory environment on small ECON slabs, rather than on a comprehensive study that allows for consideration of different shapes and sizes of electrodes. These test slabs, therefore, included only one configuration of ECON HPS, which were not easily reconfigured to test different electrode configurations. Because experimental studies are resource intensive, a finite element (FE) model of an ECON HPS test slab, developed and validated with experimental data (Sadati et al. 2017), was used to study the performance of the system under different weather conditions. It is noted that FE analysis is a commonly used method for evaluating pavement designs (Zhao et al. 2011); therefore, a field-validated FE model of ECON HPS (Sadati et al. 2018) was used as the basis for this study to evaluate performance of different design configurations.

Literature review

There have been several experimental studies related to ECON HPS (Pan et al. 2014; Wu et al. 2015; Malakooti et al. 2019), but only four are known to have previously published studies on numerical modeling of ECON HPS and only one related to electrode shape but with constant spacing (Malakooti et al. 2019). Tuan et al. (2004) performed an experimental study on the performance of heated pavements fabricated with steel shavings mixed into PCC. As a part of that study, a simplified FE model of the pavement system, including placement of the ECON layer over a regular PCC layer, was developed. While that model was used to demonstrate

that an ECON HPS system with a certain electrical resistivity had the capability to increase surface temperature under a particular set of environmental conditions, a comparison of the model's results with experimental measurements was not reported. In another study by Abdulla et al., a concrete slab including an ECON layer over a PCC layer was experimentally fabricated, and its configuration was modeled using FE. In that study, carbon fiber was added to PCC and used to fabricate the ECON. The study reported agreement at the center of the top surface with respect to measured temperature increase and resulting temperature increase reflected in the FE model. Surface temperature values were not evaluated at other surface or sub-surface locations. The validation of the studied models was limited to a laboratory experimental case that did not include modeling the heat loss from the surface resulting from melting snow and/or ice. Sadati et al. (2017, 2018) also investigated the performance of ECON HPS. In Sadati et al. (2017), FE modeling of ECON HPS for all pavement layers was performed using a model-updating method for updating the material properties of the model to improve the match between measurements and model-predicted temperature at the pavement surface. In Sadati et al. (2018), the energy and thermal performance of ECON HPS was investigated using a verified and validated FE model of ECON HPS, using typical meteorological year (TMY) data for DSM to estimate the hourly ambient temperature and daily snowfall thickness. The thermal performance of the system for typical conditions was investigated, and the energy demand of ECON HPS was compared to the energy demand of the entire DSM terminal. No previous studies have investigated the impact of different design configurations of ECON HPS on the thermal and energy performance of the system. Apart from common design parameters such as layer thickness and joint spacing, ECON HPS has a set of additional parameters that can be adjusted during the design process, including spacing between embedded electrodes, shape and dimensions of each electrode, and applied voltage. The electrode material is selected to be stainless steel, which is highly resistant to corrosion in wet environmental conditions.

Objectives and contribution

Given the significant number of ECON HPS design parameters, it is necessary to investigate the sensitivity of the system performance to the range of possible values for each of these parameters. The objective of this paper is therefore to study the individual impact of electrode shape, dimensions, and spacing design on the thermal and energy performance of ECON HPS, while other parameters are assumed to be determined by pavement design regulations for a specific application. These selected parameters, particularly important for the design of ECON HPS, are easily adjustable during the

design and construction process. This study was conducted by modifying a field-validated FE model of ECON HPS to address various design configurations while determining the predicted temperature increase at the top surface of the pavement and the associated amount of energy used. To this end, several possible electrode shape and spacing options were modeled and their thermal and energy performance was compared by defining a set of indices for evaluating system efficiency. While the methodology was applied to specifically determine the optimum design for the ECON HPS at Des Moines, Iowa, the study method and results reported in this paper could provide guidance for electrode configuration design of ECON HPS based on requirements of climate zone under associated weather conditions at other locations. The presented methodology provides a framework for energy-efficient design of ECON HPS.

The remainder of this paper describes the theoretical background, the experimental setup and measurements, the modeling methodology, and the selection of system configurations. The results of thermal and energy performance of the system under different configurations are next presented and discussed.

Theoretical background

The physical phenomenon underlying the heating process used in ECON HPS is Joule heating (Sadati et al. 2018) based on an electric potential gradient between the two ends of a conductive material. Assuming constant resistance (R), the higher the electric potential gradient (V) the higher the power of heat generation (P), as reflected by Eq. (1).

$$P = \frac{V^2}{R} \quad (1)$$

Figure 2 depicts the constant electric potential lines for the three different studied electrode shapes. The distribution of these lines depends on the geometry of the concrete material and electrodes, as well as the distance between the two electrodes. The closer the outer surfaces of the electrodes, the higher the electric potential gradient in the material.

Methodology

This section describes the experimental setup of ECON HPS test slabs at DSM and the temperature and electric current values measured during two selected snowfall events. A methodology for comparing the thermal and energy performance of different ECON HPS design configurations is developed, and performance indexes are defined accordingly.

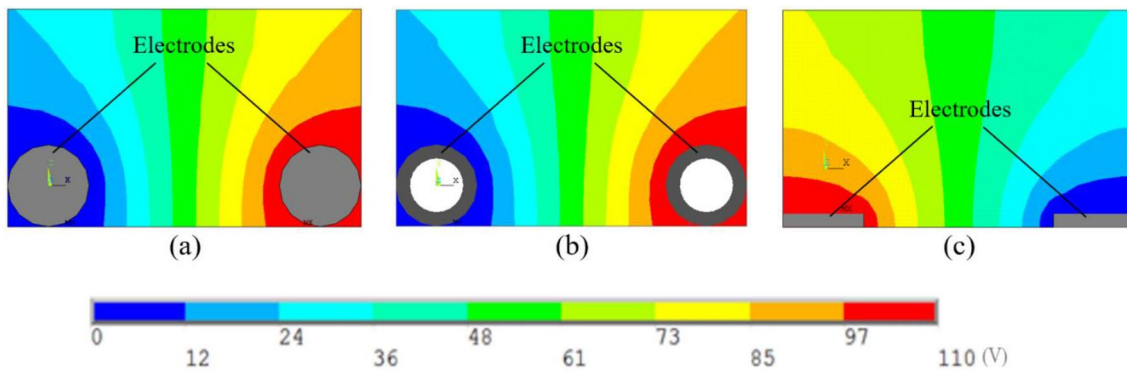


Fig. 2 Electric potential lines developed by placing electrodes with different shapes and applying electric potential difference by the electrodes, including electrode shapes of **a** solid circular bar; **b** hollow circular bar; and **c** flat bar

Experimental setup

ECON HPS test slabs built at DSM contained six electrodes embedded in their ECON layers, and a schematic illustration of the system is shown in Fig. 3. ECON HPS test slabs were 3.8 m by 4.6 m in size. The total concrete pavement thickness, including both ECON and PCC layers, was 19 cm over a base layer 20 cm thick sitting on the top of a subgrade layer. This pavement design was based on DSM requirements for the general aviation apron area.

The ECON HPS at DSM was energized during observed snowfall events. Measured values of electric current and temperature in different pavement system layers are shown in Figs. 4 and 5 for test events on December 24 and 27, 2017, respectively. It should be noted that, because of existence of electric current in the ECON layer that can interfere with the sensor readings, there are some missing values for one of the sensors located 9 cm below the pavement surface. However, considering the number of sensors

and the 10-min sampling interval, the other measured data were found to be sufficient for this study.

As shown in Figs. 4 and 5, as soon as the system is turned on, the electric current value increases, producing a continuous increase in pavement temperature, with temperatures in the deeper pavement layers initially higher than those in surface layers. Since the surface of the pavement has the largest heat loss, the sensors closest to the surface usually reflect the lowest temperatures during the winter season before the system is turned on. The thickness of ECON layer was 9 cm, and since the electrodes were placed at the bottom of this layer, the bottom of ECON layer heated faster, and the temperature at the 9 cm depth was higher than the others when the system was energized. When the system was turned off (i.e., the current value drops to zero), the pavement temperature begins to decrease faster at the surface because of the heat loss due to convection.



Fig. 3 Schematic illustration of the pavement layers for electrically conductive heated pavement system test slabs built at Des Moines International Airport

Fig. 4 Electric current and temperature variations in different layers of the pavement and the ambient temperature on December 24, 2017

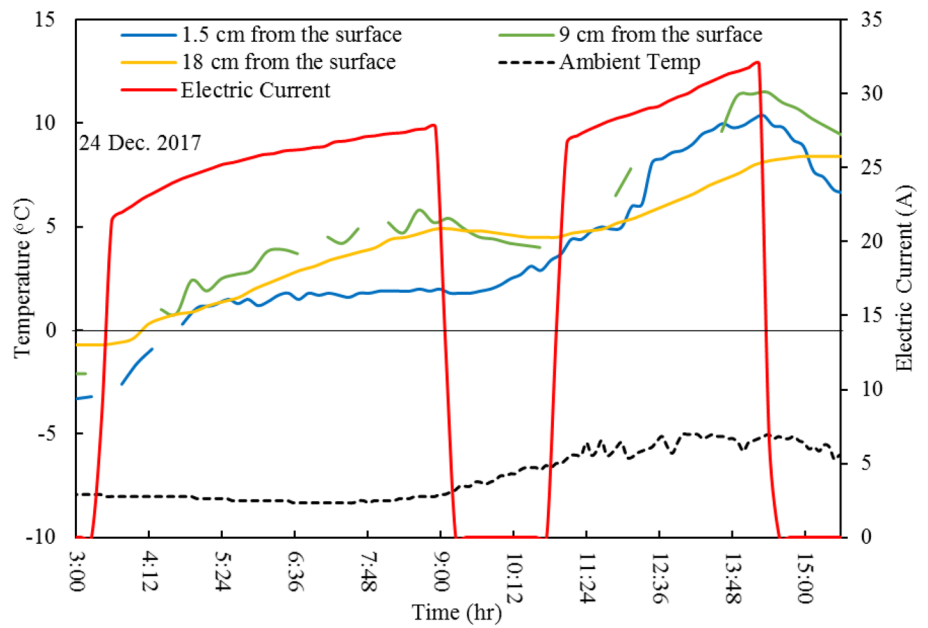
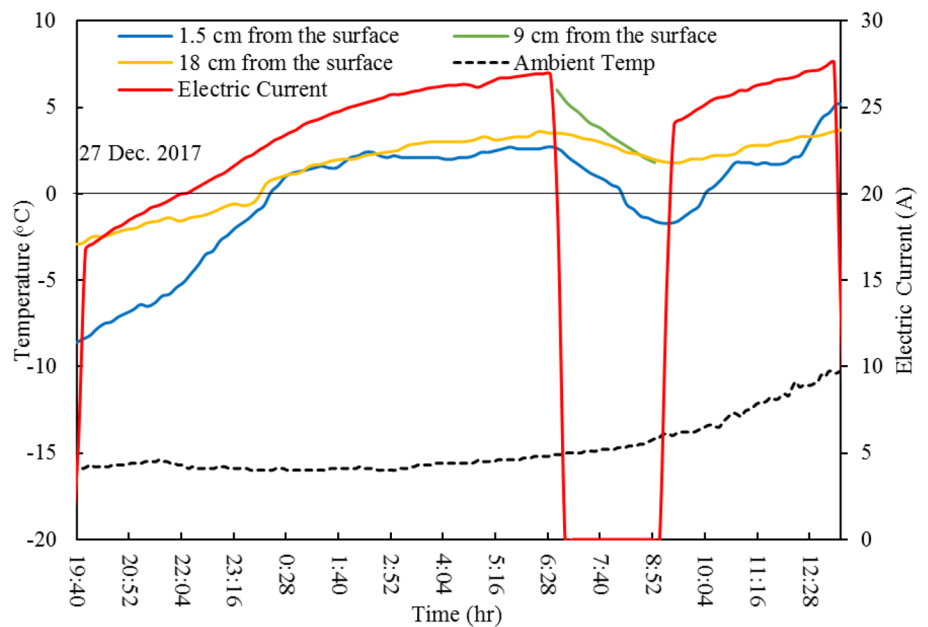


Fig. 5 Electric current and temperature variations in different layers of the pavement and ambient temperature on December 27, 2017



Finite element model

An FE model was developed in ANSYS Inc. (2018) and validated with experimental data, as described in studies by Sadati et al. (2017, 2018). The modeled loads and boundary conditions used are shown in Fig. 6.

The governing equations for the resistive heating process are (Liu 2017):

$$E = -\nabla\phi, \tag{2}$$

$$J = \frac{1}{\rho}E, \tag{3}$$

$$\nabla \cdot J = 0, \tag{4}$$

where E is the electric field (V/m), ϕ is the electric potential (V), J is the electric current density (A/m^2), and ρ is the electrical resistivity ($\Omega\cdot m$). Transient thermal analysis for simulating the heating process that produces temperature variation by time is based on the following equations (Liu 2017):

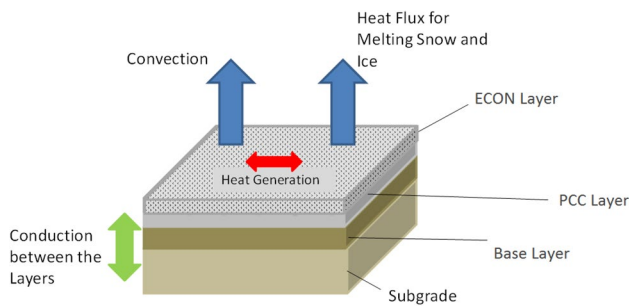


Fig. 6 The model is capable of simulating all pavement layers including the heat generation in ECON layer and heat transfer between different pavement layers and the interaction between the surface and the environment

$$q'' = -k\nabla T \tag{5}$$

$$k\nabla^2 T + \dot{q} = \beta C_p \frac{\partial T}{\partial t} \tag{6}$$

$$\dot{q} = \rho |J|^2, \tag{7}$$

where q'' is the heat flux (W/m^2), k is the thermal conductivity ($W/m \text{ } ^\circ C$), T is the temperature ($^\circ C$), \dot{q} is the heat generation by Joule heating (W/m^3), β is the mass density (kg/m^3), C_p is the specific heat ($J/kg \text{ } ^\circ C$), and t is time (s).

In the FE model, since the temperature (T) varies in both space and time (ANSYS Inc. 2018), the temperature at each node is considered to be dependent on time and T can be calculated by multiplying element shape functions to the nodal temperature vectors of Eq. (8),

$$T = \{N\}^T \{T_n\} \tag{8}$$

where $\{N\}$ is a space-dependent element shape function vector and $\{T_n\}$ is the time-dependent nodal temperature vector of each element.

For a transient solution, with a constant voltage, the FE equation for this problem can be written as

$$\begin{bmatrix} C & 0 \\ 0 & 0 \end{bmatrix} \begin{bmatrix} \dot{T} \\ \phi \end{bmatrix} + \begin{bmatrix} K^t & 0 \\ 0 & K^e \end{bmatrix} \begin{bmatrix} T \\ \phi \end{bmatrix} = \begin{bmatrix} Q \\ I \end{bmatrix} \tag{9}$$

where I is the electric current, Q is the heat flux, C is the specific heat coefficient, K^t is the thermal conductivity, and K^e is the electrical conductivity. The time derivatives of T can be written as

$$\dot{T} = \frac{\partial T}{\partial t} \{N\}^T \{T_n\}. \tag{10}$$

Because of the symmetry of the model, to study the impact of electrode size and shape on thermal and energy performance, a 2D FE model using shell elements was developed using the methodology described in Sadati et al. (2018). The validated FE model was then modified to simulate the performance of each of the design configurations described in Table 1. These ten configurations with various electrode spacing, shapes and dimensions were modeled, and their energy and thermal performances are compared. To ensure that the modeled materials are available and the defined configurations only include options that are technically feasible for pavement construction, the values for electrode spacing and the shape and dimensions of the electrodes, given in Table 1, are determined based on the recommendations based on discussions with DSM and Iowa Department of Transportation (DOT) engineers.

Section IDs were assigned to various configurations using designations “XY-Z.D,” where X is the number of electrodes in the section, Y is the electrode shape (C for circular, H for hollow circular, and F for flat), and $Z.D$ is the outer diameter (mm) in the case of circular/hollow circular. For the flat bar case, Z is the width and D stands for the thickness, both in mm. Electrode spacing was defined as the center-to-center distance between each pair of electrodes. Three different electrode

Table 1 Design configurations simulated by FE model to compare their performance

Test section #	Section ID	Number of electrodes (spacing)	Size of electrode cross section	Electrode type and shape
1	10C-20	10 (500 mm)	Diameter 20 mm	Smooth circular bar
2	10F-25.3	10 (500 mm)	Width and thickness 25 mm×3 mm	Flat bar
3	10H-25	10 (500 mm)	Diameter 25 mm	Hollow circular bar
4	10C-25	10 (500 mm)	Diameter 25 mm	Smooth circular bar
5	8C-20	8 (650 mm)	Diameter 20 mm	Smooth circular bar
6	8C-25	8 (650 mm)	Diameter 25 mm	Smooth circular bar
7	8F-25.3	8 (650 mm)	Width and thickness 25 mm×3 mm	Flat bar
8	8H-25	8 (650 mm)	Diameter 25 mm	Hollow circular bar
9	6C-20	6 (900 mm)	Diameter 20 mm	Smooth circular bar
10	6C-25	6 (900 mm)	Diameter 25 mm	Smooth circular bar

spacing values, each for electrodes with various shapes and sizes, were modeled as follows: (i) 50 cm with 10 electrodes, (ii) 60 cm with 8 electrodes, and (iii) 100 cm with 6 electrodes embedded. For each configuration, a comparison of surface temperature showed the ability to generate heat and operate under a range of climate conditions and snow event severity.

Each configuration was simulated by applying 240 VAC between each pair of electrodes. All other conditions were kept the same for all configurations since the purpose of the simulation is to determine the effect of electrode shape, dimension, and spacing on the thermal and energy performance of the system.

FE model elements for all pavement layers in the model, for a configuration including eight solid circular electrodes with 8150 elements, are shown in Fig. 7. The time step used for the transient analysis was 5 min. Both the number of elements and the time step were checked to assure the convergence of results.

Performance evaluation method

The criteria used for comparing the performance of the evaluated system configurations consisted of two metrics—the rate of change of the temperature and the amount of power input to the system for heat generation. Equations (11) and (12) describe these two metrics as the *thermal performance index (TI)* and *energy performance index (EI)*:

$$TI = \frac{\Delta T}{\Delta t_m} \quad (11)$$

$$EI = \frac{\bar{P} \times \Delta t_h}{\Delta t_m} \quad (12)$$

where ΔT (°C) is the pavement surface temperature increase during the time interval Δt_m (min) and \bar{P} (kW) is the average power input of the system during the given time of Δt_m (min)

and Δt_h (h). \bar{P} is multiplied with Δt_h to estimate the total amount of energy input in (kWh). The overall performance of the system is described by *performance index (PI)* as shown in Eq. (13).

$$PI = \frac{TI}{EI} \quad (13)$$

Since the goal of this design is to increase the pavement surface temperature to the desired point with the minimum amount of power input, a higher value of *PI* indicates a better system performance. A higher *PI* coefficient shows that a higher portion of the input energy is used for increasing the temperature of the pavement surface, the ultimate goal of the design of ECON HPS.

Results and discussion

A total time of 120 min was used in performing the simulation. The temperature distribution and power input obtained for each design configuration are given in Table 1. Contour plots of the temperature distribution for test Sections 1, 7, and 10 are shown in Fig. 8 as sample configurations with 10, 8, and 6 embedded electrodes, respectively. Other configurations exhibited similar temperature patterns with different temperature values.

The estimated average surface temperature increase with time for each design configuration is shown in Fig. 9, and the estimated power input is shown in Fig. 10. As shown in these figures, both thermal and energy performance changed significantly with changes in electrode spacing. It is also observed that a greater number of electrodes increase the power input to the slabs and the resulting energy consumption. It should be noted that in order to adjust this energy consumption, the voltage applied to each pair of electrodes

Fig. 7 Finite element model of an ECON HPS configuration with eight solid stainless steel circular electrodes

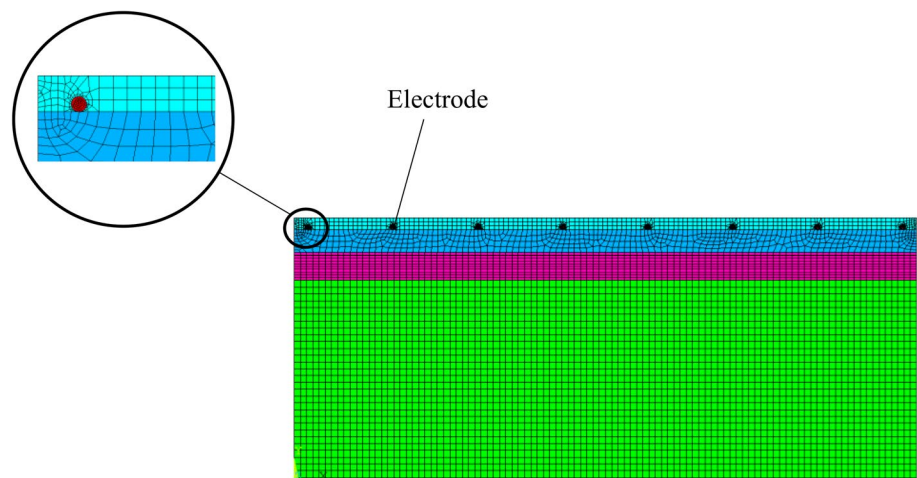


Fig. 8 Temperature distribution of three of the design configurations with 10 (Test Section 1, circular 20 mm diameter), 8 (Test Section 7, flat 25 mm×3 mm), and 6 (Test Section 10, circular 25 mm diameter) electrodes

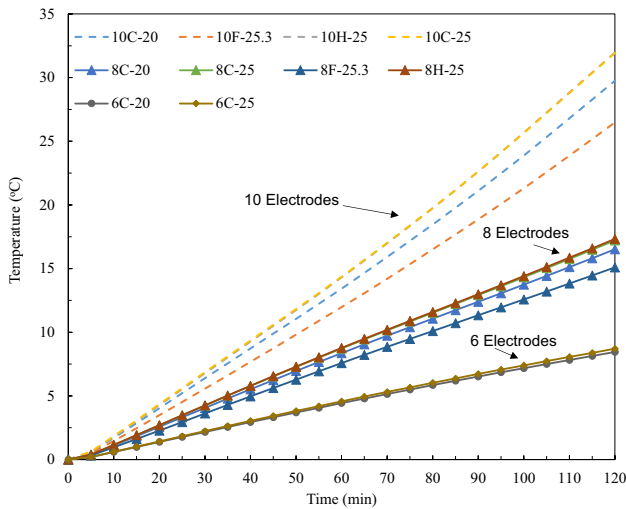
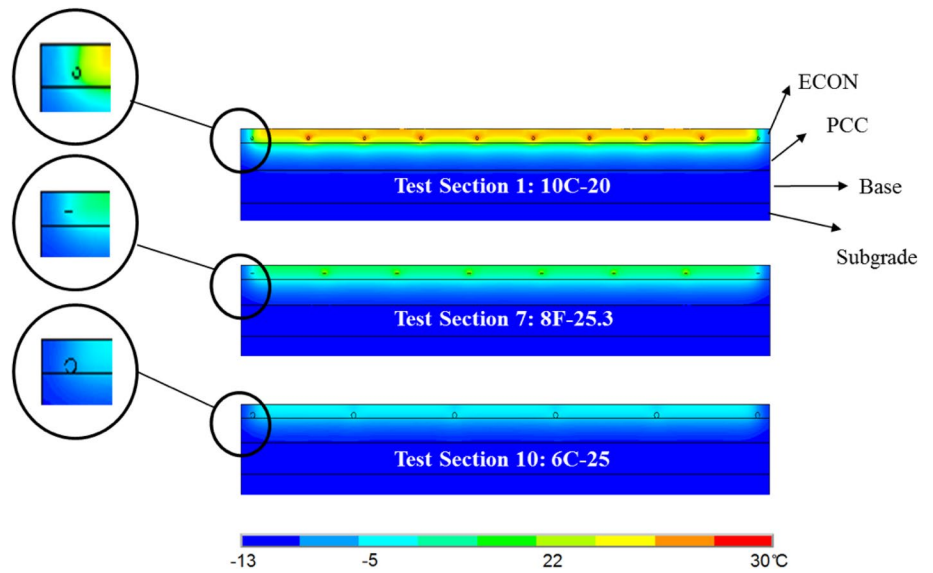


Fig. 9 Estimated average surface temperature increase in each electrode configuration over time (Section IDs are assigned to different configurations as “XY-Z.D” where X stands for the number of electrodes in the section, Y stands for the shape of the electrodes (“C” for “circular,” “H” for “hollow circular,” and “F” for “flat”), and Z.D stands for the diameter (mm) in case of “circular”/“hollow circular” and width (Z) plus thickness (D) (mm) in case of flat bars.)

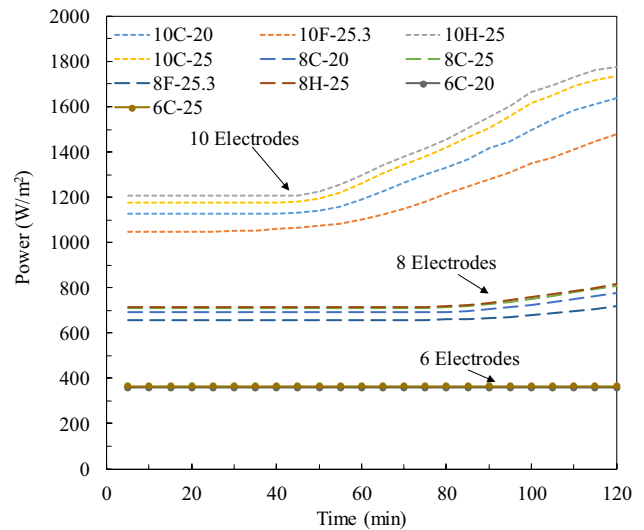


Fig. 10 Estimated power density of each electrode configuration (Section IDs are assigned to different configurations as “XY-Z.D” where X stands for the number of electrodes in the section, Y stands for the shape of the electrodes (“C” for “circular,” “H” for “hollow circular,” and “F” for “flat”) and Z.D stands for the diameter (mm) in case of “circular”/“hollow circular” and width (Z) plus thickness (D) (mm) in case of flat bars.)

could also be adjusted; however, this was not within the scope of evaluation of this effort.

Figure 11 provides a comparison of the performance of each design configuration based on the calculated PI value. As shown, Test Section 10 (6C-25) had the highest PI value and exhibited the best performance among the simulated design configurations. On the other hand, Test Section 2 (10F-25.3) and 7 (8F-25.3) had the lowest PI values, indicating that, for a given amount of energy input, these design configurations resulted in lower surface temperature

increases than all other studied configurations. Electrodes in Test Section 10 were 25-mm-diameter circular bars, representing the largest cross sections among all electrodes. Electrodes with the smallest cross section area (flat bars) were used in Test Sections 2 and 7. Therefore, the electrode cross section, which significantly impacts the voltage in the ECON layer, is an important factor in the system performance. While Test Section 10, with 6 electrodes at 100 cm spacing, had a lower surface temperature increase compared

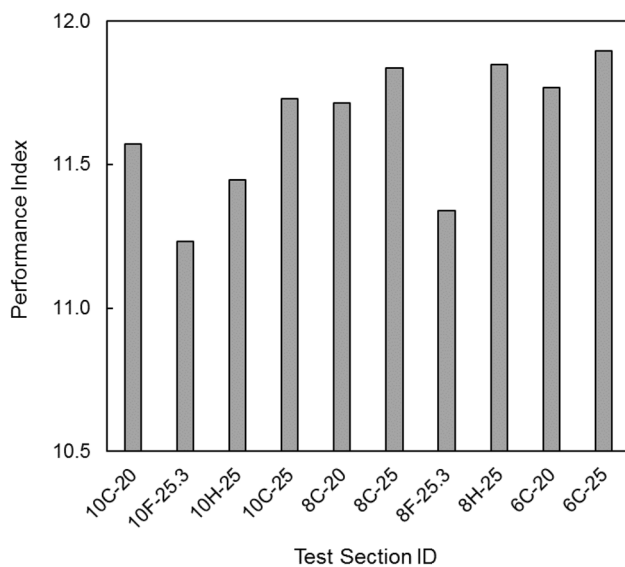


Fig. 11 Performance index for each configuration based on the results of the finite element simulations

to a section with 10 electrodes at 50 cm spacing (Fig. 9), the portion input energy used to increase the surface temperature for Test Section 10 was higher than for all other sections. As such, Test Section 10 achieved higher efficiency in terms of input energy used for increasing the average surface temperature.

A higher *PI* value indicates the capability of a system to increase the average pavement surface temperature for 1 kWh of consumed energy. Although the variation in the *PI* values shown in Fig. 11 is small, it can make a considerable difference with respect to overall energy consumption if there are a large number of constructed ECON HPS slabs. For example, if 1,000 equal-sized slabs were constructed for a project, choosing a configuration with a *PI* value of 0.5 units larger results in saving 1 MWh of energy for each 0.5° C increase at the average pavement surface in an hour. Therefore, the selection of an energy-efficient design would considerably help with reducing the energy demand for this system, which results in a less environmental impact. It should be noted, however, that the *PI* value should not be treated as the sole criteria for choosing among the configuration options. While a higher *PI* value indicates that a configuration has a higher average temperature at the pavement surface for a given amount of energy input, it does not guarantee generation of the required weather-dependent heat flux. Therefore, regional energy requirements should be considered for a reliable performance of a heated pavement, as reported by ASHRAE (2009). For example, based on the ASHRAE Fundamentals Handbook, the required heat flux values for melting snow on pavement in Iowa and Massachusetts for 99% of their snow events are approximately 340 W/m² and 550 W/m², respectively. Thus, considering

the system power shown in Fig. 10, a configuration with 6 electrodes at 100 cm spacing could work for Iowa, while in Massachusetts, based on historical climate conditions, the designed configuration should either have 8 electrodes at 60 cm or smaller spacing.

The results of this study demonstrate the significance of electrode shape, dimension, and spacing in designing an ECON HPS configuration. Although it is seen that increasing the number of electrodes can increase the amount of energy consumption and a higher temperature can be achieved, the configuration can be further optimized for obtaining an efficient system in terms of energy demand. This is particularly significant when one considers the necessity of reducing the overall energy consumption of infrastructure (Kilkiş and Kilkiş 2016).

Conclusions

To establish a framework for the energy-efficient design of electrically conductive concrete (ECON) heated pavement system (HPS), ten design configurations for ECON HPS were modeled based on a field data-validated finite element (FE) model. Each configuration had a unique electrode shape, dimension, and spacing based on recommendations by Des Moines International Airport and Iowa Department of Transportation engineers. The models for each configuration were simulated using the same operational conditions. These are the main findings of this study:

- Performance index (*PI*) is introduced as a measure of the energy efficiency of ECON HPS to evaluate the thermal and energy performance of this system. The relative value of this index reflects the capability of the system to increase the pavement surface temperature in a given time and with a given amount of energy. Since a higher value of *PI* indicates that a higher portion of the input energy is consumed for increasing the surface temperature, it is reflective of the efficiency of the system.
- Configurations were compared for their efficiency based on *PI* values.
- A configuration with 6 circular electrodes at 100 cm spacing exhibited the highest *PI* value, and the results indicated that a higher electrode cross-sectional area would result in a higher *PI* value.
- Although the study of *PI* value provides insight into performance of different system configurations, the regional energy requirements for heated pavement systems based on the weather conditions should also be investigated as the subject for future studies.

This study provides the framework for energy-efficient design of ECON HPS and to evaluate the effectiveness of

this framework in the field; further experimental tests should be undertaken in future studies.

Acknowledgements The authors would like to thank the Iowa Department of Transportation (DOT) and the Iowa Highway Research Board (IHRB) for providing the matching funds for this research project which is sponsored by the Federal Aviation Administration (FAA). The authors would also like to thank the FAA Air Transportation Center of Excellence for the Partnership to Enhance General Aviation Safety, Accessibility and Sustainability (PEGASAS). The IHRB technical advisory committee (TAC) members from Iowa DOT and Iowa Counties, particularly Mr. Mike Harvey, Director of Iowa DOT's Support Services Office Administrative Services Division, and Iowa DOT electricians, the FAA PEGASAS Technical Monitor for Heated Airport Pavements project, and Mr. Gary L. Mitchell of the American Concrete Pavement Association (ACPA) are gratefully acknowledged for their guidance, support, and direction throughout the research. The authors would like to express their sincere gratitude to other research team members from ISU's Program for Sustainable Pavement Engineering and Research (PROSPER) at Institute for Transportation for their assistance with the laboratory and field investigations. Although the Iowa DOT and FAA have sponsored this study, they neither endorse nor reject the findings of this research. This paper does not constitute a standard, specification, or regulation.

References

- Abdualla H, Ceylan H, Kim S et al (2016) System requirements for electrically conductive concrete heated pavements. *Transp Res Rec* 2569:70–79
- Abdualla H, Ceylan H, Kim S, et al (2018) Design and construction of the first full-scale electrically conductive concrete heated airport pavement system at a US Airport
- Abdualla H, Gopalakrishnan K, Ceylan H, et al (2017) Development of a finite element model for electrically conductive concrete heated pavements. the 96th Annual meeting of Transportation Research Board, January 8–12, 2017, Washington, DC, pp 1–18
- Amini K, Vosoughi P, Ceylan H, Taylor P (2019) Linking air-void system and mechanical properties to salt-scaling resistance of concrete containing slag cement. *Cem Concr Compos* 104:103364. <https://doi.org/10.1016/j.cemconcomp.2019.103364>
- Anand P, Ceylan H, Gkritza KN, et al (2014) Establishing parameters for cost comparison of alternative airfield snow removal methodologies. The 2014 FAA Worldwide Airport Technology Transfer Conference, August 5-7, 2014, Galloway, New Jersey
- ANSYS Inc. (2018) ANSYS®
- ASHRAE (2007) International Climate Zone Definitions
- ASHRAE (2009) Snow melting and freeze protection. In: ASHRAE handbook: fundamentals, 15th edn. American Society of Heating, Refrigerating and Air-Conditioning Engineers, Atlanta, GA
- Fay L, Honarvarnazari M, Jungwirth S, et al (2015) Manual of environmental best practices for snow and ice control
- Jiang W, Xiao J, Yuan D et al (2018) Design and experiment of thermoelectric asphalt pavements with power-generation and temperature-reduction functions. *Energy Build* 169:39–47. <https://doi.org/10.1016/j.enbuild.2018.03.049>
- Kilkiş B, Kilkiş Ş (2016) New exergy metrics for energy, environment, and economy nexus and optimum design model for nearly-zero exergy airport (nZEXAP) systems. *Energy* 140:1–21. <https://doi.org/10.1016/j.energy.2017.04.129>
- Liu TJC (2017) Numerical analysis of joule heating behaviour and residual compressive stress around crack tip under high electric load. *Model Simul Eng* 2017:1–9. <https://doi.org/10.1155/2017/3012949>
- Malakooti A (2017) Investigation of concrete electrical resistivity as a performance based test. Utah State University
- Malakooti A, Abdualla H, Sassani A, et al (2019) Effect of electrode geometry and size on heating performance of electrically conductive concrete (19–02535). In: Transportation Research Board (TRB) 99th Annual Meeting. Washington, D.C.
- Malakooti A, Maguire M, Thomas RJ (2018) Evaluating electrical resistivity as a performance based test for Utah bridge deck concrete (CAIT-UTC-NC35). Rutgers Univ Cent Adv Infrastruct Transp
- Pan P, Wu S, Xiao F et al (2014) Conductive asphalt concrete: a review on structure design, performance, and practical applications. *J Intell Mater Syst Struct* 26:755–769. <https://doi.org/10.1177/1045389X14530594>
- Sadati SMS, Cetin K, Ceylan H et al (2018) Energy and thermal performance evaluation of an automated snow and ice removal system at airports using numerical modeling and field measurements. *Sustain Cities Soc* 43:238–250. <https://doi.org/10.1016/j.scs.2018.08.021>
- Sadati SMS, Cetin K, Ceylan H (2017) Numerical modeling of electrically conductive pavement systems. In: Congress on technical advancement 2017. ASCE, Duluth, MN, pp 1–10
- Sassani A, Arabzadeh A, Ceylan H et al (2018) Carbon fiber-based electrically conductive concrete for salt-free deicing of pavements. *J Clean Prod* 203:799–809. <https://doi.org/10.1016/j.jclepro.2018.08.315>
- Shamsaei M, Khafajeh R, Aghayan I (2019) Laboratory evaluation of the mechanical properties of roller compacted concrete pavement containing ceramic and coal waste powders. *Clean Technol Environ Policy* 21:707–716. <https://doi.org/10.1007/s10098-018-1657-5>
- Tuan CY (2004) Concrete technology today: conductive concrete for bridge deck deicing. Nebraska Department of Roads
- Voskamp IM, Van de Ven FHM (2015) Planning support system for climate adaptation: Composing effective sets of blue-green measures to reduce urban vulnerability to extreme weather events. *Build Environ* 83:159–167. <https://doi.org/10.1016/j.buildenv.2014.07.018>
- Wu J, Liu J, Yang F (2015) Three-phase composite conductive concrete for pavement deicing. *Constr Build Mater* 75:129–135. <https://doi.org/10.1016/j.conbuildmat.2014.11.004>
- Zhao Y, Liu X, Scarpas A et al (2011) Numerical analysis of integral pavement/soil-wall structures in soft soil. *Finite Elem Anal Des* 47:461–469. <https://doi.org/10.1016/j.finel.2010.12.010>

Publisher's Note Springer Nature remains neutral with regard to jurisdictional claims in published maps and institutional affiliations.

Affiliations

S. M. Sajed Sadati¹  · Kristen S. Cetin²  · Halil Ceylan^{3,4}  · Sunghwan Kim⁵ 

S. M. Sajed Sadati
ssadati@iastate.edu

Halil Ceylan
hceylan@iastate.edu

Sunghwan Kim
sunghwan@iastate.edu

¹ Civil, Construction and Environmental Engineering,
Intelligent Infrastructure Engineering, Iowa State University,
Ames, IA, USA

² Civil and Environmental Engineering, Michigan State
University, East Lansing, MI, USA

³ Civil, Construction and Environmental Engineering,
Partnership To Enhance General Aviation Safety,
Accessibility and Sustainability (PEGASAS), Federal
Aviation Administration (FAA) Center of Excellence (COE)
On General Aviation, Iowa State University, Ames, IA, USA

⁴ Program for Sustainable Pavement Engineering & Research
(PROSPER), Iowa State University, Ames, IA, USA

⁵ Institute for Transportation, Iowa State University, Ames, IA,
USA